Scientific Research Publishing

Circuits and Systems, 2024, 15, 29-43
https://www.scirp.org/journal/cs
ISSN Online: 2153-1293
ISSN Print: 2153-1285

Robust Nonlinear Current Sensorless Control of the Boost Converter with Constant Power Load

Said Oucheriah, Abul Azad

Department of Engineering Technology, Northern Illinois University, DeKalb, IL, United States
Email: soucheria@niu.edu, aazad@niu.edu

How to cite this paper: Oucheriah, S. and Azad, A. (2024) Robust Nonlinear Current Sensorless Control of the Boost Converter with Constant Power Load. *Circuits and Systems*, **15**, 29-43.
https://doi.org/10.4236/cs.2024.153003

Received: January 16, 2024
Accepted: March 26, 2024
Published: March 29, 2024

Abstract

The boost converter feeding a constant power load (CPL) is a non-minimum phase system that is prone to the destabilizing effects of the negative incremental resistance of the CPL and presents a major challenge in the design of stabilizing controllers. A PWM-based current-sensorless robust sliding mode controller is developed that requires only the measurement of the output voltage. An extended state observer is developed to estimate a lumped uncertainty signal that comprises the uncertain load power and the input voltage, the converter parasitics, the component uncertainties and the estimation of the derivative of the output voltage needed in the implementation of the controller. A linear sliding surface is used to derive the controller, which is simple in its design and yet exhibits excellent features in terms of robustness to external disturbances, parameter uncertainties, and parasitics despite the absence of the inductor's current feedback. The robustness of the controller is validated by computer simulations.

Keywords

Boost Converter, Robust Sliding Mode Control, Constant Power Load (CPL), Current-Sensorless Control, Extended State Observer

1. Introduction

Nowadays, power electronic converters are extensively used in power distribution systems and they are usually cascaded. Some of these converters operate as tightly regulated loads that absorb constant power and behave as constant power loads (CPLs). These loads exhibit negative incremental impedances that can lead to serious destabilizing effects on the input source which may be another DC-DC

converter and present a major challenge in the design of stabilizing robust controllers for the supply converters.

Numerous design techniques have been published in the literature to regulate the output voltage of DC-DC converters to counter the instability effects of the CPL-induced negative impedance such as passive damping [1] and active damping [2]. A technique that uses nonlinear feedback to cancel the destabilizing effect of CPL, also known as the loop cancellation technique is presented in [3] and a control method based on a linearization via state feedback is used in [4].

Sliding mode control (SMC) has been extensively used for DC-DC converters and has been proven to yield a robust nonlinear control scheme against parameter uncertainties and external disturbances. A PWM-based SMC is developed in [5] to regulate the output voltage of the buck-boost converter feeding a CPL. The proposed control law suffers from chattering effects as shown in the simulation and experimental plots. An SMC is proposed in [6] that uses a sliding surface that is a linear combination of the errors of both inductor current and capacitor voltage with respect to their respective steady-state values. The proposed controller leads to a small value of inrush current. However, the controller suffers from variable switching frequency effects. The implementation of both SMC controllers requires four sensors to measure the input voltage, the inductor current, the capacitor voltage and the CPL current.

When the load power is unknown, we may have to resort to robust controllers that require some type of estimation scheme. The authors in [7] proposed an adaptive passivity-based controller to regulate the output voltage of the DC-DC buck-boost converter feeding an unknown CPL. The resulting controller is very complicated and, therefore, is impractical for real applications. To remedy the complexity of the control law, a simpler modified controller is developed in [8] by using a change of coordinate and partial linearization that transforms the system into a cascade form. However, the approach relies on the time-scaled model that presents problems in practical applications. An adaptive passivity-based controller that does not use time scaling or any kind of linearization technique is provided in [9] with a complete stability analysis of the nonlinear system. However, the controller still seems to be complicated and strongly dependent on the converter parameters to be of any practical interest. In [10], a controller was developed to regulate the output voltage of the DC-DC boost converter feeding an unknown CPL that was estimated using a nonlinear differential equation. However, the controller does not account for input voltage variations, parasitics and parameter uncertainties. In [11], an observer-based sliding mode control for the boost converter feeding a CPL was proposed to ensure the finite-time stability of the closed-loop system. In this study, only the input voltage is assumed unknown and is estimated using a finite-time observer to adjust a controller parameter. Only step reference changes and step input changes are tested in simulation and the robustness of the controller to parasitics, parameter uncertainties and output load power changes are neither tested or accounted for in the design of the controller. In [12], the cumulative losses of the converter are modelled as a resistor

in series with the inductor and its value with the value of the load power are estimated using the immersion and variance technique and both incorporated in the controller design. However, the input voltage disturbances and parameter uncertainties are not accounted for in the controller design. In [13], a passivity-based control is proposed to regulate the output voltage of an unknown constant power load fed by a boost converter. The CPL is estimated using the immersion and invariance technique, and a disturbance observer is used to estimate the input voltage of the converter. In [14], an adaptive nonlinear controller based on a nonlinear disturbance observer and passivity-based control is proposed to ensure the stability of a buck-boost converter in a DC microgrid in the presence of disturbances and uncertainties.

Ignoring parasitics, parameter uncertainties, and input voltage and output load power disturbances in the controller's design may result in a degradation of the output response. In this case, the output response may suffer from substantial steady-state errors with large output variations when the converters are subject to large unknown time-varying load power and input voltage variations. We should note that the implementation of the controllers listed here relies on at least two sensors, the inductor current and the output voltage, and in some implementations, four sensors are required. Recently, there has been an interest in the use of current sensorless controllers to reduce the cost and to improve the reliability and miniaturization of the device.

To address the above limitations, a PWM-based current-sensorless robust sliding mode controller for the DC-DC boost converter feeding a CPL is proposed that takes into account the uncertainties of the component values, the unknown parasitics of the converters, the unknown input voltage and load power variations. The implementation of the controller requires only the measurement of the output voltage. To the author's best knowledge, the use of only one sensor to measure the output voltage for the design of a stabilizing controller for the boost converter driving a CPL has not appeared in the literature. An extended state estimator is developed to estimate a lumped disturbance signal that includes external disturbances, uncertainties, and parasitics and also to estimate the derivative of the output voltage that is used in the controller feedback instead of the measured inductor current. A linear sliding surface is used to derive the controller and a simple stability analysis of the nonlinear closed-loop system is presented instead of the traditional linearized one used for local stability. The controller design is very simple and yet is capable of dynamically compensating for the disturbance to achieve a very high performance in terms of disturbance rejection without feedback from the inductor current. The effectiveness of the proposed controller is validated by simulation.

2. Robust Nonlinear Current-Sensorless Control Design

2.1. Averaged Model of Boost Converter with CPL and Parasitics

A basic boost converter with parasitic elements feeding a CPL is shown in **Figure 1**.

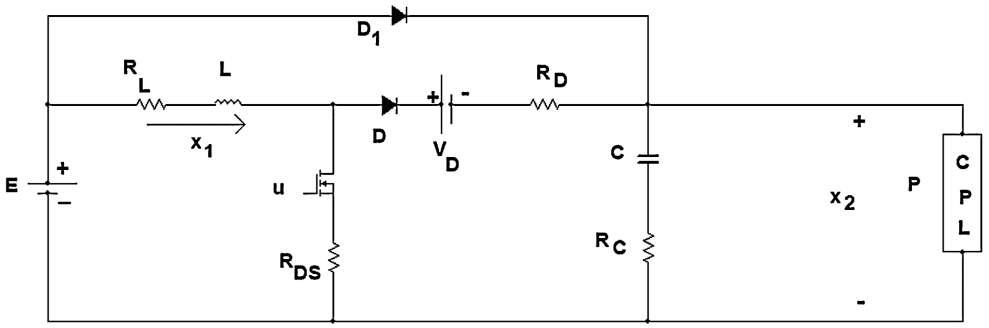

Figure 1. A boost converter with basic parasitics feeding a CPL.

Under continuous conduction mode (CCM), the averaged model of the boost converter including parasitic components, is derived using Kirchhoffs circuit laws in both modes and then using the state-space averaging technique to obtain

$$\begin{aligned}\dot{x}_1 &= -\left(\frac{R_L}{L}+\frac{R_{DS}}{L}u+(1-u)\frac{R_D}{L}\right)x_1-(1-u)\frac{x_2}{L}-(1-u)\frac{V_D}{L}+\frac{E}{L}\\ \dot{x}_2 &= (1-u)\frac{x_1}{C}-\frac{P}{Cx_2}+(1-u)R_C\dot{x}_1+\frac{R_CP}{x_2^2}\dot{x}_2\end{aligned} \tag{1}$$

where x_1 represents the average inductor current and $x_2 \in \mathbb{R} > 0$ is the average capacitor voltage. The unknown parameters E, L, C and P represent the input voltage, the inductance, the capacitance and the power respectively. However, their respective nominal values E_o, L_o, C_o and P_o are assumed to be known for the implementation of the controller. The control input u to the converter is the duty ratio function. The unknown parameters R_L, R_{DS}, R_D, V_D and R_C represent the inductor equivalent series resistance, the MOSFET on-resistance, the diode forward resistance, the conducting voltage of the diode and the capacitor equivalent series resistance respectively. The switching losses could have been accounted for by including a switching loss resistance in the inductor branch as proposed in [15]. During the start-up phase and neglecting the parasitics, the diode D_1 guarantees that the initial condition

$$x_2(0) = E \tag{2}$$

and the reduction of the inrush current in the inductor [10].

System (1) can be written as

$$\begin{aligned}\dot{x}_1 &= u\frac{x_2}{L_o}+d_1\\ \dot{x}_2 &= (1-u)\frac{x_1}{C_o}+d_2\end{aligned} \tag{3}$$

where

$$\begin{aligned}d_1 &= -\left(\frac{R_L}{L}+\frac{R_{DS}}{L}u+(1-u)\frac{R_D}{L}\right)x_1-\frac{x_2}{L}-(1-u)\frac{V_D}{L}+\frac{E}{L}+\left(\frac{1}{L}-\frac{1}{L_o}\right)ux_2\\ d_2 &= (1-u)\left(\frac{1}{C}-\frac{1}{C_o}\right)x_1-\frac{P}{Cx_2}+(1-u)R_C\dot{x}_1+\frac{R_CP}{x_2^2}\dot{x}_2\end{aligned} \tag{4}$$

Taking the derivative of both sides of the second equation of (3) and using the expression for $\dot{x}_1$ given by the first equation of (3) yields

$$\begin{aligned}\ddot{x}_2 &= (1-u)\frac{\dot{x}_1}{C_o} - \dot{u}\frac{x_1}{C_o} + \dot{d}_2 \\ &= u(1-u)\frac{x_2}{L_oC_o} + (1-u)\frac{d_1}{C_o} - \dot{u}\frac{x_1}{C_o} + \dot{d}_2\end{aligned} \tag{5}$$

System 5 can be rewritten as

$$\ddot{x}_2 = \frac{u}{L_oC_o}x_2 + d \tag{6}$$

where the uncertain lumped signal d is given by

$$d = -\frac{u^2}{L_oC_o}x_2 + \frac{1-u}{C_o}d_1 - \dot{u}\frac{x_1}{C_o} + \dot{d}_2 \tag{7}$$

Assumption: The first derivative of the lumped uncertainties is bounded by $\delta > 0$ with

$$\left|\dot{d}\right| \le \delta = \sup_{t\in[0,\infty)}\left|\dot{d}(t)\right| \tag{8}$$

Such assumption is required for the synthesis of stabilizing controllers for DC-DC converters and is assumed in many studies [16]-[19].

Let

$$\begin{aligned}e_2 &= x_2 - V_{ref} \\ e_1 &= \dot{e}_2\end{aligned} \tag{9}$$

Using the substitution $x_2 = e_2 + V_{ref}$, $\dot{x}_2 = e_1$ and $\ddot{x}_2 = \dot{e}_1$ into (6), model (1) can be redefined as

$$\begin{aligned}\dot{e}_1 &= \frac{u}{L_oC_o}\left[e_2 + V_{ref}\right] + d \\ \dot{e}_2 &= e_1\end{aligned} \tag{10}$$

2.2. Design of the Extended State Observer

By using the lumped uncertainty d as a state variable, the extended observer (ESO) for the system (10) is

$$\begin{aligned}\dot{q}_1 &= \frac{u}{L_oC_o}\left[e_2 + V_{ref}\right] + q_3 + K_3e_2 - K_1q_1 - K_1^2e_2 \\ \dot{q}_2 &= q_1 + K_1e_2 + K_2\tilde{q}_2 \\ \dot{q}_3 &= -K_3q_1 - K_1K_3e_2 \\ \hat{e}_1 &= q_1 + K_1e_2,\ \hat{e}_2 = q_2 \\ \hat{d} &= q_3 + K_3e_2,\ \tilde{q}_2 = e_2 - q_2\end{aligned} \tag{11}$$

where $\hat{e}_1, \hat{e}_2$ and $\hat{d}$ are the estimates of e_1, e_2 and d respectively. The parameters K_1, K_2 and K_3 are the observer gains. Using (10) and (11), the dynamics of the state errors are

$$\begin{aligned}\dot{\tilde{e}}_1 &= -K_1\tilde{e}_1 + \tilde{d}\\ \dot{\tilde{e}}_2 &= \tilde{e}_1 - K_2\tilde{e}_2\\ \dot{\tilde{d}} &= -K_3\tilde{e}_1 + \dot{d}\end{aligned} \tag{12}$$

which can be written in compact form as

$$\dot{\tilde{e}} = A\tilde{e} + B\dot{d} \tag{13}$$

with

$$A = \begin{bmatrix} -K_1 & 0 & 1\\ 1 & -K_2 & 0\\ -K_3 & 0 & 0\end{bmatrix},\ B = \begin{bmatrix}0\\0\\1\end{bmatrix} \tag{14}$$

and where $\tilde{e}_1 = e_1 - \hat{e}_1$, $\tilde{e}_2 = e_2 - \hat{e}_2$, $\tilde{d} = d - \hat{d}$ and $\tilde{e} = \left[\tilde{e}_1, \tilde{e}_2, \tilde{d}\right]^{\mathrm{T}}$.

The eigenvalues of the system matrix A are determined from the characteristic equation

$$s^3 + \left(K_1 + K_2\right)s^2 + \left(K_1K_2 + K_3\right)s + K_2K_3 = 0 \tag{15}$$

There always exists K_1, K_2 and K_3 such that the poles are on the left-half side of the complex plane with the matrix A being Hurwitz. In this case, for any matrix $Q = Q^{\mathrm{T}} > 0$, there exists a unique solution $P = P^{\mathrm{T}} > 0$ satisfying the Lyapunov equation

$$A^{\mathrm{T}}P + PA = -Q \tag{16}$$

Consider the Lyapunov function

$$V\left(\tilde{e}\right) = \tilde{e}^{\mathrm{T}}P\tilde{e} \tag{17}$$

Its derivative along the solutions of (13) yields

$$\begin{aligned}\dot{V} &= -\tilde{e}^{\mathrm{T}}Q\tilde{e} + 2\tilde{e}^{\mathrm{T}}PB\dot{d}\\ &\le -\lambda_{\min}Q\left\|\tilde{e}\right\|^2 + 2\left\|P\right\|\left\|B\right\|\left\|\tilde{e}\right\|\delta\end{aligned} \tag{18}$$

and the observer estimation error $\tilde{e}$ is bounded by ϵ given by

$$\left\|\tilde{e}\right\| \le \epsilon = 2\frac{\left\|P\right\|\delta}{\lambda_{\min}\left(Q\right)} \tag{19}$$

where δ is defined in (8) and $\lambda_{\min}\left(Q\right)$ denotes the minimum eigenvalue of Q.

2.3. Design of the Controller and Stability Analysis

We consider the following sliding surface

$$\begin{aligned}\sigma &= \hat{e}_1 + \gamma\hat{e}_2 - K_1e_2\\ &= q_1 + \gamma q_2\end{aligned} \tag{20}$$

where we have used $\hat{e}_1 = q_1 + K_1e_2$ and $q_2 = \hat{e}_2$ and $\gamma > 0$ is a design parameter. We consider the following controller

$$u = \alpha\left(K_1 - \gamma\right)q_1 - \alpha q_3 + \alpha(K_1^2 - K_3 - \gamma K_1)e_2 - \alpha K_2\gamma\tilde{q}_2 - \alpha K_4\sigma \tag{21}$$

where

$$\alpha = \frac{L_o C_o}{e_2 + V_{ref}} \tag{22}$$

Using (20), the controller (21) is derived by differentiating σ with respect to time and setting $\dot{\sigma} = 0$. The last term $\alpha K_4 \sigma$ is added to ensure the sliding mode condition.

The substitution of the controller (21) into the derivative of (20) leads to

$$\dot{\sigma} = -K_4 \sigma \tag{23}$$

Therefore, we have $\dot{\sigma}\sigma = -K_4 \sigma^2 < 0$ which ensures the sliding mode condition. Equation (23) admits as a solution

$$\sigma(t) = \sigma(0) \mathrm{e}^{-K_4 t} \tag{24}$$

Using the initial conditions $q_1(0) = 0$, $q_2(0) = 0$ for the extended state estimator (11) yields $\sigma(0) = 0$ and in this case $\sigma(t) = 0$ for all $t \geq 0$ with the reaching phase completely eliminated.

Theorem 1: For the system (1) with the extended state estimator (11) and driven by the controller (21), the output voltage x_2 is uniformly convergent to a ball $\Omega(r)$ centered at V_{ref} with a radius r given by

$$r = \frac{(\gamma + 1)\epsilon}{\gamma - K_1} \tag{25}$$

with a decay rate $(\gamma - K_1)$. Here $\gamma > K_1$ and the parameter ϵ is defined in (19).

Proof: Substituting $(e_1 - \tilde{e}_1)$ for $\hat{e}_1$, $(e_2 - \tilde{e}_2)$ for $\hat{e}_2$ and $\sigma = 0$ in equation(20) and solving for e_1 yields

$$e_1 = -(\gamma - K_1) e_2 + \tilde{e}_1 + \gamma \tilde{e}_2 \tag{26}$$

Using $e_1 = \dot{x}_2$ and $e_2 = x_2 - V_{ref}$ into (26) yields the following dynamic equation

$$\dot{x}_2 = -(\gamma - K_1)(x_2 - V_{ref}) + \tilde{e}_1 + \gamma \tilde{e}_2 \tag{27}$$

In view of (19), $\|\tilde{e}_1\| \leq \epsilon$, $\|\tilde{e}_2\| \leq \epsilon$ and the solution x_2 of (27) is bounded by

$$x_2 \leq \left[V_{ref} + \frac{(\gamma + 1)\epsilon}{\gamma - K_1} \right] \left(1 - \mathrm{e}^{-(\gamma - K_1)t} \right) \tag{28}$$

and consequently, x_2 is uniformly convergent to a ball centered at V_{ref} with a radius r given by (25) and a decay rate $(\gamma - K_1)$.

Remark: If the lumped uncertainty d is bounded and satisfies $\lim_{t \to \infty} \dot{d} = 0$ then $\tilde{e}_1, \tilde{e}_2$ and $\tilde{d}$ converge asymptotically to 0 with x_2 exponentially converging to V_{ref} with a decay rate $(\gamma - K_1)$. In some situations where we have only step load power and and step input voltage changes then we may have $\dot{d} \approx 0$ long after the onset of the step changes.

Taking into account the parasitics of the converter, it is easily shown that the inductor current x_1 converges to

$$x_1 \to x_{1f} = \frac{-b - \sqrt{b^2 - 4ac}}{2a} \tag{29}$$

and the controller u to

$$u \to 1 - \frac{P}{x_{1f} V_{ref}} \tag{30}$$

where

$$\begin{aligned} &a = V_{ref}\left(R_L + R_{DS}\right),\ b = \left(PR_D - PR_{DS} - EV_{ref}\right) \\ &c = P\left(V_D + V_{ref}\right) \end{aligned} \tag{31}$$

In the absence of parasitics we have

$$\begin{aligned} &x_1 \to x_{1f} = \frac{P}{E} \\ &u \to 1 - \frac{E}{V_{ref}} \end{aligned} \tag{32}$$

Shown in Figure 2, is the block diagram of the proposed current-sensorless robust sliding mode controller.

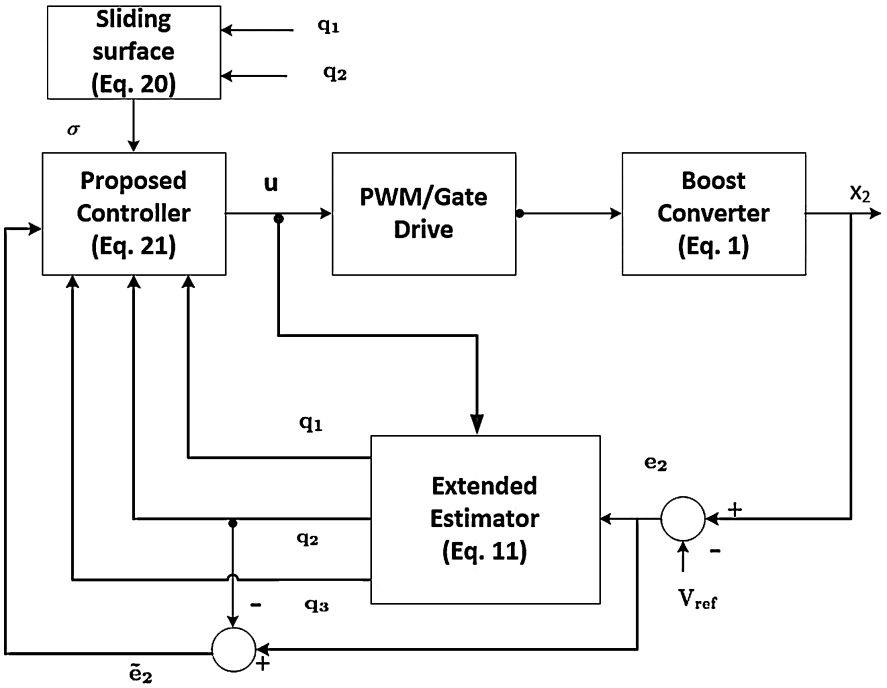

Figure 2. Block diagram of the proposed robust sliding mode controller.

3. Simulation Results

The actual DC-DC boost converter parameters that are unknown to the designer are

$$\begin{aligned} &E = 20\ \text{V},\ L = 180\ \mu\text{H},\ C = 150\ \mu\text{F} \\ &P = 50\ \text{W},\ V_{ref} = 60\ \text{V} \end{aligned} \tag{33}$$

To test the robustness of the proposed controller, the following nominal parameters that are known to the designer are used

$$E_o = 24\ \text{V},\ L_o = 90\ \mu\text{H},\ C_o = 300\ \mu\text{F}$$
$$P_o = 40\ \text{W},\ V_{ref} = 60\ \text{V} \tag{34}$$

To account for the conduction losses, we consider the parasitics of the boost converter as

$$R_L = 0.2\,\Omega,\ R_{DS} = 0.01\,\Omega,\ V_D = 0.7\ \text{V},\ R_D = 0.4\,\Omega,\ R_C = 0.1\,\Omega \tag{35}$$

The simulations are performed using the switched model with a switching frequency of 200 kHz instead of the averaged model.

The gains of the estimator/controller parameters are chosen as

$$\gamma = 20\times10^3,\ K_1 = 100,\ K_2 = 250\times10^3,$$
$$K_3 = 250\times10^3,\ K_4 = 1 \tag{36}$$

The initial conditions of the extended estimator $q_1(0) = 0$, $q_2(0) = 0$ and $q_3(0) = 0$.

Case 1: Figure 3 depicts the time evolution of the output voltage x_2 when the converter is subject to a step reference change from 60 V to 80 V at 0.2 s and from 80 V to 60 V at 0.4 s. Figure 4 and Figure 5 depict the inductor current x_1 and the duty ratio u, respectively.

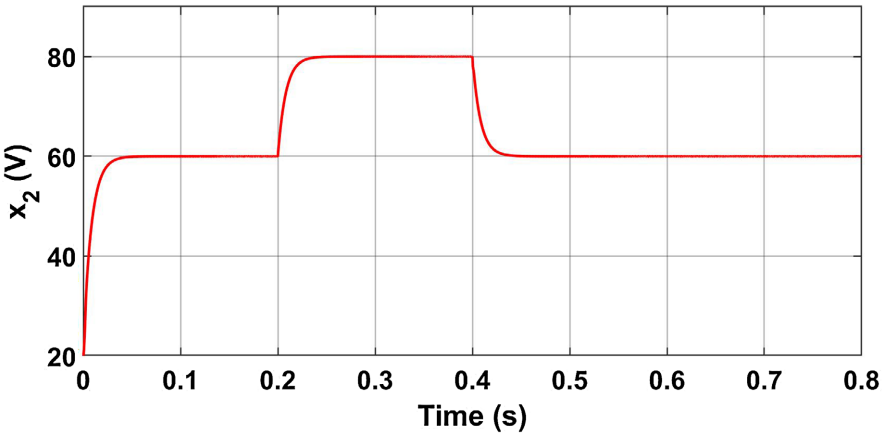

Figure 3. Output voltage response of the converter due to step voltage reference changes.

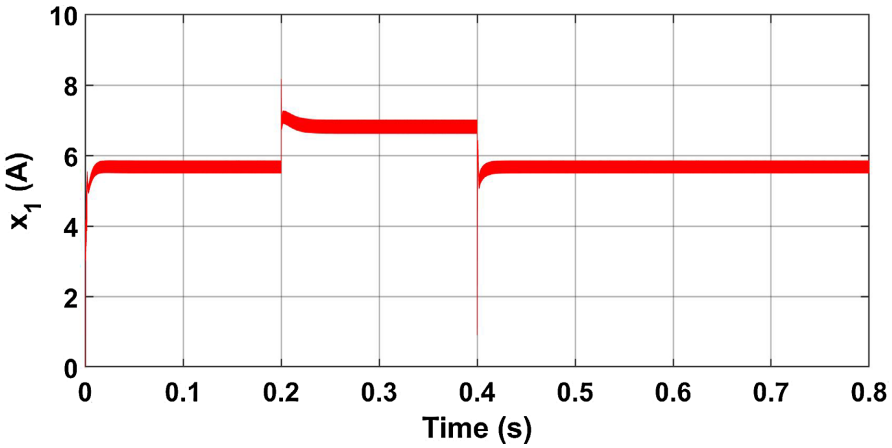

Figure 4. Inductor current.

Case 2: For the load power disturbance rejection test, the converter is subject to the time-varying load power profile shown in Figure 6 with $E = 20$ V and $V_{ref} = 60$ V. Figure 7 shows the time evolution of the output voltage x_2. Figure 8 and Figure 9 depict the inductor current x_1 and the duty ratio u, respectively.

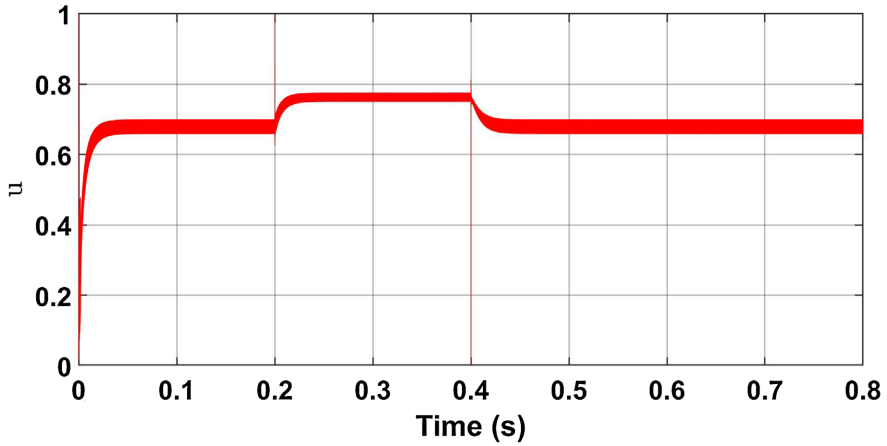

Figure 5. Duty ratio u.

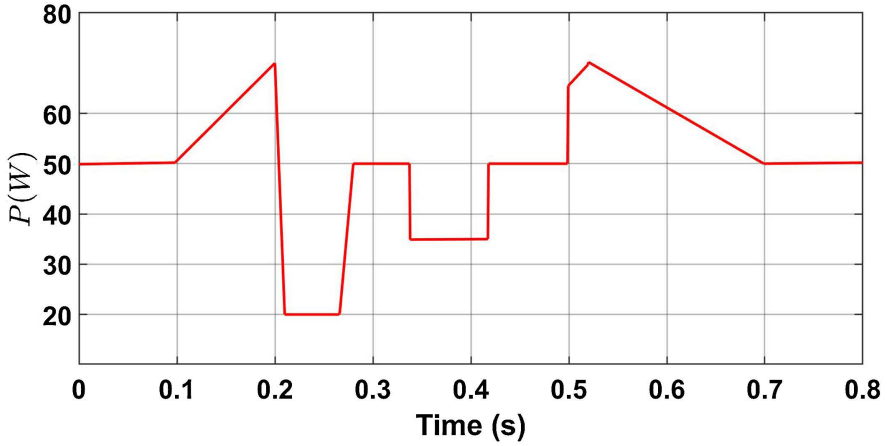

Figure 6. Load power variation.

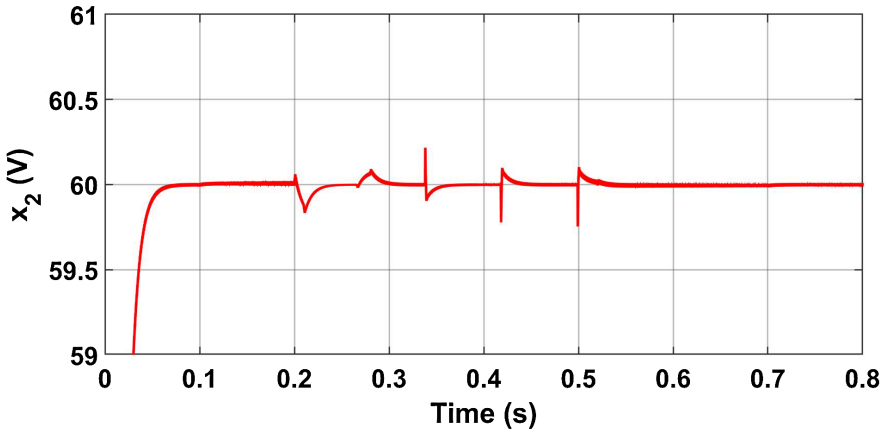

Figure 7. Output voltage response of the converter due to load power changes.

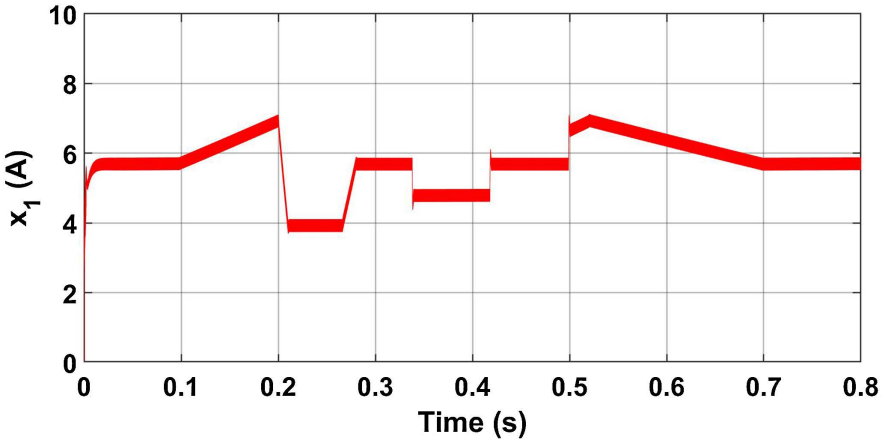

Figure 8. Inductor current.

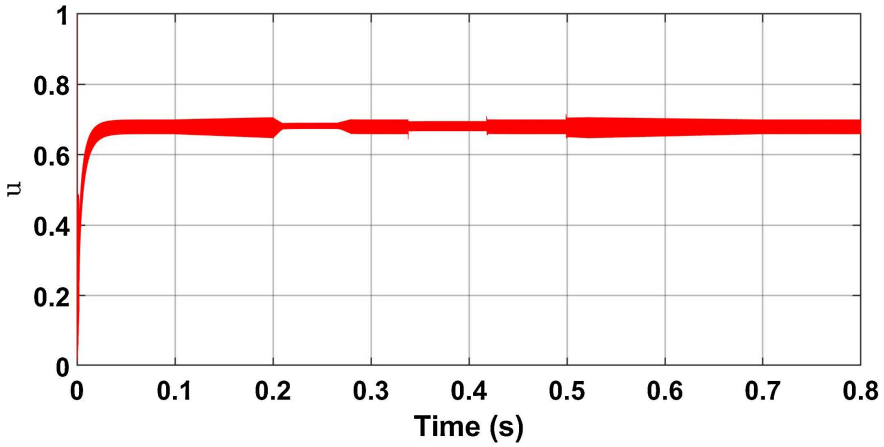

Figure 9. Duty ratio u.

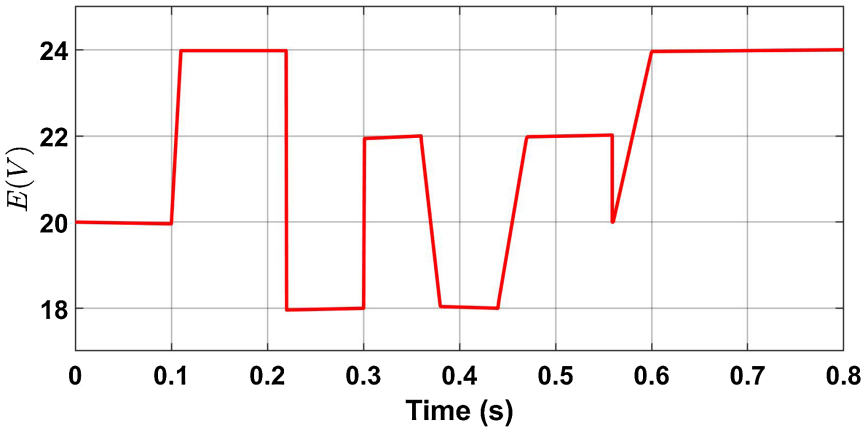

Figure 10. Input voltage variation.

Case 3: For the input voltage disturbance rejection test, the converter is subject to the time-varying input voltage profile shown in Figure 10 with $P = 50$ W and $V_{ref} = 20$ V. Figure 11 shows the time evolution of the output voltage x_2. Figure 12 and Figure 13 depict the inductor current x_1 and the duty ratio u, respectively.

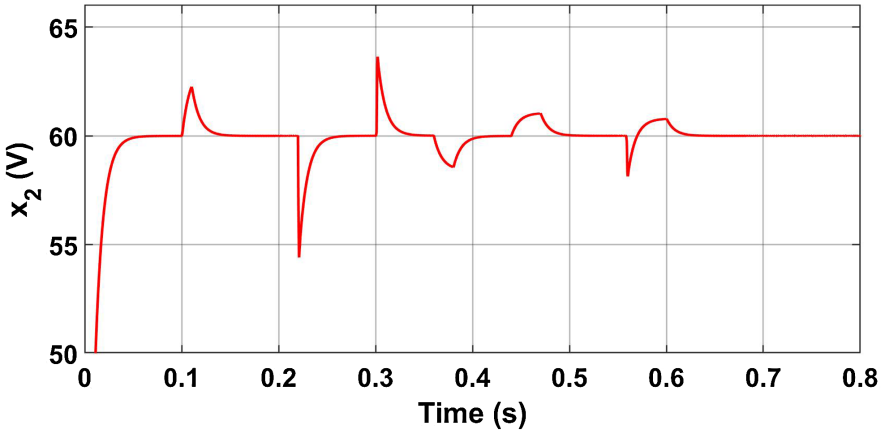

Figure 11. Output voltage response of the converter due to input voltage changes.

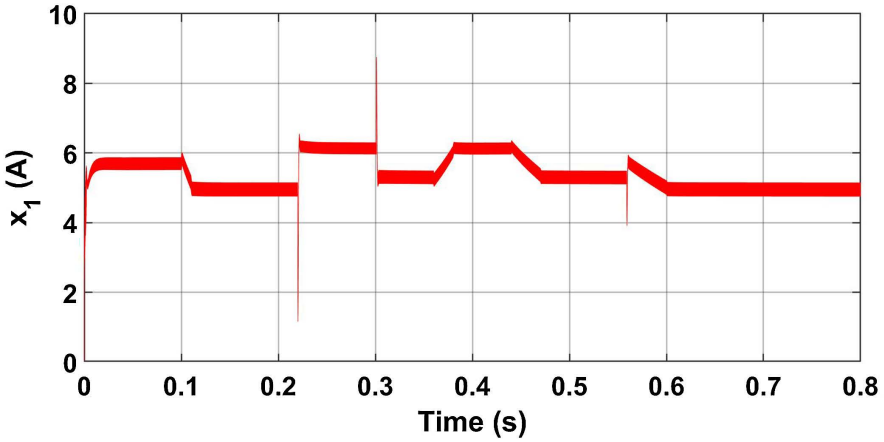

Figure 12. Inductor current.

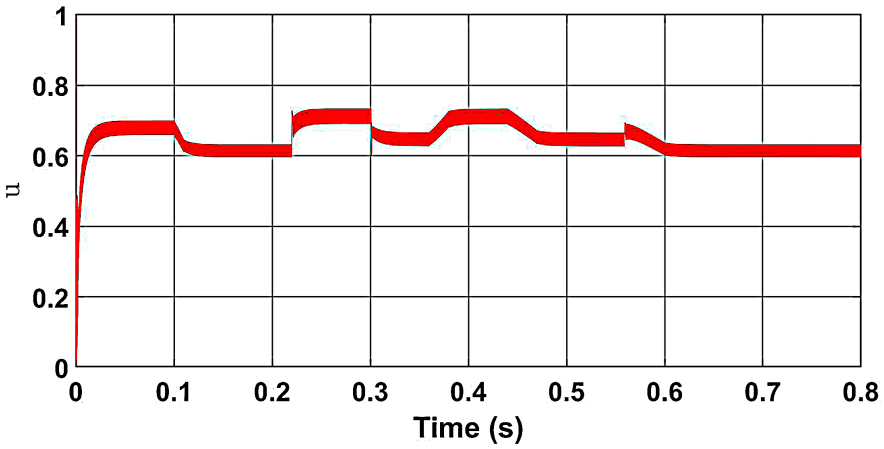

Figure 13. Duty ratio *u*.

Case 4: For the robustness of the controller to noise test, the load power profile of case 2 is corrupted by noise with a maximum amplitude of 3. All the pertinent values of Case 2 are maintained. Figure 14 depicts the noisy output load power profile and Figure 15 shows the corresponding output response.

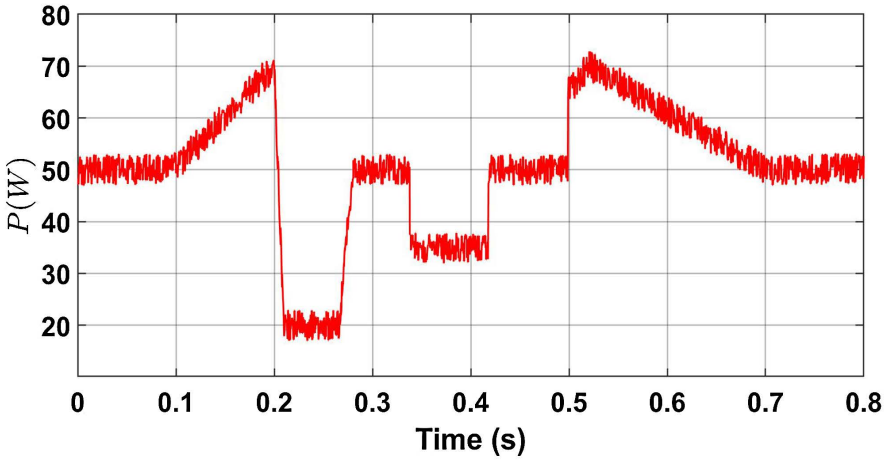

Figure 14. Load power variation with noise.

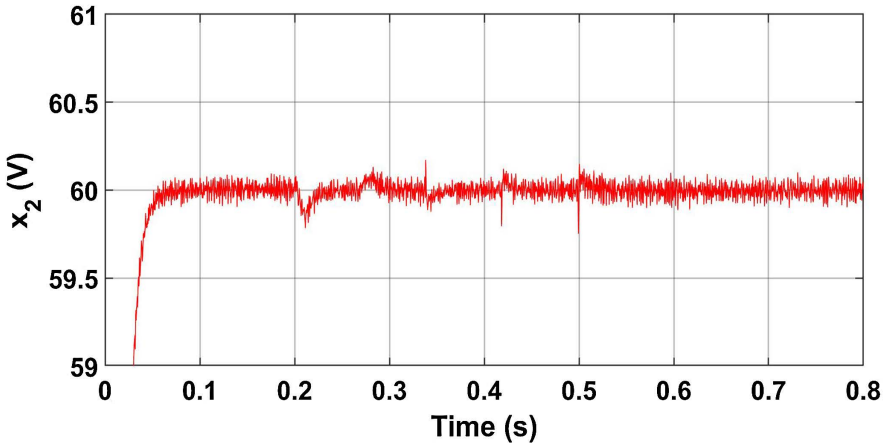

Figure 15. Output voltage response of the converter due to load power changes with noise.

As seen in these simulation results, the proposed controller exhibits an excellent disturbance suppression capability during load power and input voltage changes with small overshoots and short recovery time.

4. Conclusion

A PWM-based current-sensorless robust sliding mode controller for the DC-DC boost converter with CPL is proposed that requires only one sensor for the output voltage measurement. An extended state observer is used to estimate a lumped uncertainty signal that comprises the uncertain power load, the input voltage, parameter uncertainties, and parasitics, as well as to estimate the derivative of the output voltage. A linear sliding surface is used to derive the controller. The proposed controller is simple in its design yet exhibits excellent features in disturbances suppression despite the absence of current feedback from the inductor. Its robustness is validated by computer simulations. Future work will be the validation of these results experimentally and the development of a simple procedure to systematically determine the controller's parameters.

Conflicts of Interest

The authors declare no conflicts of interest regarding the publication of this paper.

References

[1] Cespedes, M., Xing, L. and Sun, J. (2011) Constant-Power Load System Stabilization by Passive Damping. *IEEE Transactions on Power Electronics*, **26**, 1832-1836. https://doi.org/10.1109/tpel.2011.2151880

[2] Rahimi, A.M. and Emadi, A. (2009) Active Damping in DC/DC Power Electronic Converters: A Novel Method to Overcome the Problems of Constant Power Loads. *IEEE Transactions on Industrial Electronics*, **56**, 1428-1439. https://doi.org/10.1109/tie.2009.2013748

[3] Rahimi, A.M., Williamson, G.A. and Emadi, A. (2010) Loop-Cancellation Technique: A Novel Nonlinear Feedback to Overcome the Destabilizing Effect of Constant-Power Loads. *IEEE Transactions on Vehicular Technology*, **59**, 650-661. https://doi.org/10.1109/tvt.2009.2037429

[4] Sulligoi, G., Bosich, D., Giadrossi, G., Zhu, L., Cupelli, M. and Monti, A. (2014) Multiconverter Medium Voltage DC Power Systems on Ships: Constant-Power Loads Instability Solution Using Linearization via State Feedback Control. *IEEE Transactions on Smart Grid*, **5**, 2543-2552. https://doi.org/10.1109/tsg.2014.2305904

[5] Singh, S., Rathore, N. and Fulwani, D. (2016) Mitigation of Negative Impedance Instabilities in a DC/DC Buck-Boost Converter with Composite Load. *Journal of Power Electronics*, **16**, 1046-1055. https://doi.org/10.6113/jpe.2016.16.3.1046

[6] Martinez‐Treviño, B.A., El Aroudi, A., Vidal-Idiarte, E., Cid-Pastor, A. and Martinez-Salamero, L. (2019) Sliding-Mode Control of a Boost Converter under Constant Power Loading Conditions. *IET Power Electronics*, **12**, 521-529. https://doi.org/10.1049/iet-pel.2018.5098

[7] He, W., Ortega, R., Machado, J.E. and Li, S. (2018) An Adaptive Passivity-Based Controller of a Buck-Boost Converter with a Constant Power Load. *Asian Journal of Control*, **21**, 581-595. https://doi.org/10.1002/asjc.1751

[8] He, W., Soriano-Rangel, C.A., Ortega, R., Astolfi, A., Mancilla-David, F. and Li, S. (2018) Energy Shaping Control for Buck–Boost Converters with Unknown Constant Power Load. *Control Engineering Practice*, **74**, 33-43. https://doi.org/10.1016/j.conengprac.2018.02.006

[9] Soriano-Rangel, C.A., He, W., Mancilla-David, F. and Ortega, R. (2021) Voltage Regulation in Buck–Boost Converters Feeding an Unknown Constant Power Load: An Adaptive Passivity-Based Control. *IEEE Transactions on Control Systems Technology*, **29**, 395-402. https://doi.org/10.1109/tcst.2019.2959535

[10] Martinez-Trevino, B.A., Aroudi, A.E., Valderrama-Blavi, H., Cid-Pastor, A., Vidal-Idiarte, E. and Martinez-Salamero, L. (2021) PWM Nonlinear Control with Load Power Estimation for Output Voltage Regulation of a Boost Converter with Constant Power Load. *IEEE Transactions on Power Electronics*, **36**, 2143-2153. https://doi.org/10.1109/tpel.2020.3008013

[11] He, W. and Shang, Y. (2022) Finite-Time Parameter Observer-Based Sliding Mode Control for a DC/DC Boost Converter with Constant Power Loads. *Electronics*, **11**, Article No. 819. https://doi.org/10.3390/electronics11050819

[12] Oucheriah, S. (2022) Nonlinear Control of the Boost Converter Subject to Unknown Constant Power Load and Parasitics. *International Journal of Electronics Letters*, **11**, 30-40. https://doi.org/10.1080/21681724.2021.2025438

[13] Riffo, S., Gil-González, W., Montoya, O.D., Restrepo, C. and Muñoz, J. (2022) Adaptive Sensorless Pi$^+$ Passivity-Based Control of a Boost Converter Supplying an Unknown CPL. *Mathematics*, **10**, Article No. 4321. https://doi.org/10.3390/math10224321

[14] Abdolahi, M., Adabi, J. and Mousazadeh Mousavi, S.Y. (2024) Implementation and Control of a Buck–Boost Converter Connected to a Constant Power Load in a DC Microgrid. *Electrical Engineering*. https://doi.org/10.1007/s00202-024-02538-x

[15] Ayachit, A. and Kazimierczuk, M.K. (2019) Averaged Small-Signal Model of PWM DC-DC Converters in CCM Including Switching Power Loss. *IEEE Transactions on Circuits and Systems II*: *Express Briefs*, **66**, 262-266. https://doi.org/10.1109/tcsii.2018.2848623

[16] Tian, Z., Lyu, Z., Yuan, J. and Wang, C. (2019) Ude-Based Sliding Mode Control of DC–DC Power Converters with Uncertainties. *Control Engineering Practice*, **83**, 116-128. https://doi.org/10.1016/j.conengprac.2018.10.019

[17] Kim, S. and Lee, K. (2022) Current-Sensorless Energy-Shaping Output Voltage-Tracking Control for DC/DC Boost Converters with Damping Adaptation Mechanism. *IEEE Transactions on Power Electronics*, **37**, 9266-9274. https://doi.org/10.1109/tpel.2022.3159793

[18] Errouissi, R., Shareef, H., Viswambharan, A. and Wahyudie, A. (2022) Disturbance-Observer-Based Feedback Linearization Control for Stabilization and Accurate Voltage Tracking of a DC–DC Boost Converter. *IEEE Transactions on Industry Applications*, **58**, 6687-6700. https://doi.org/10.1109/tia.2022.3183040

[19] Linares-Flores, J., Juarez-Abad, J.A., Hernandez-Mendez, A., Castro-Heredia, O., Guerrero-Castellanos, J.F., Heredia-Barba, R., *et al.* (2022) Sliding Mode Control Based on Linear Extended State Observer for DC-to-DC Buck-Boost Power Converter System with Mismatched Disturbances. *IEEE Transactions on Industry Applications*, **58**, 940-950. https://doi.org/10.1109/tia.2021.3130017